

## Development of the CASL-VERA V4.2m5 MPACT 51-group Libraries with ENDF/B-VII.0 and VII.1

Kang Seog Kim<sup>1</sup>, Mark L. Williams<sup>1</sup>, Dorothea Wiarda<sup>1</sup>, Kevin T. Clarno<sup>1</sup>, and Yuxuan Liu<sup>2</sup>

<sup>1</sup>Oak Ridge National Laboratory, 1 Bethel Valley Rd., Oak Ridge, TN 37831, USA  
kimk1@ornl.gov; williamsml@ornl.gov; wiardada@ornl.gov; clarnokt@ornl.gov

<sup>2</sup>Department of Nuclear Science and Engineering, University of Michigan: 2355 Bonisteel Blvd. Ann Arbor, MI, 48105  
yuxuanl@umich.edu

**Abstract** - The MPACT neutronics module of the Consortium for Advanced Simulation of Light Water Reactors (CASL) core simulator is a 3-D whole core transport code being developed for the CASL toolset, Virtual Environment for Reactor Analysis (VERA). The v4.1m3 MPACT 47-group library with ENDF/B-VII.0, which was developed previously by using Oak Ridge National Laboratory AMPX/SCALE code packages, includes deficiencies, especially for burnt fuel cases. New v4.2m5 MPACT 51-group libraries with ENDF/B-VII.0 and VII.1 have been developed to have better accuracy by improving the library generation methodology. This study discusses a detailed procedure to generate the MPACT 51-group libraries and results for various benchmark problems.

### I. INTRODUCTION

The MPACT [1] neutronics module of the Consortium for Advanced Simulation of Light Water Reactors (CASL) [2] core simulator is a 3-D whole core transport code being developed for the CASL toolset, Virtual Environment for Reactor Analysis (VERA). MPACT is under development for neutronics simulation coupled with the CTF code for thermal-hydraulics simulation for pressurized light water reactors. Key characteristics of the MPACT code include (1) a subgroup method for resonance self-shielding and (2) a whole-core transport solver with a 2-D/1-D synthesis method. Thus the MPACT code requires a cross-section library to support all the MPACT core simulation capabilities.

The MPACT cross-section library has been generated based on the AMPX/SCALE code packages [3] developed at Oak Ridge National Laboratory with additional programs and procedures that are being developed to generate subgroup data, transient data, epithermal upscattering resonance data, and the final MPACT format library, which is not supported by the AMPX/SCALE code packages.

New AMPX and MPACT 51-group libraries with the ENDF/B-VII.0 and VII.1 nuclear data have been generated for the CASL MPACT neutronics module. The new 51-group structure was developed to be a subset of the SCALE-6.2 [3] 252-group structure and to be applicable for both pressurized water reactor (PWR) and boiling water reactor (BWR) applications. Currently, the primary scattering calculation option of the VERA-CS MPACT module is a transport-corrected  $P_0$ . Therefore, the 51-group structure has been developed for group widths to be evenly distributed to minimize convergence issues in whole-core transport calculations.

Several deficiencies have been identified in the previous MPACT 47-group library [4]. Deficiencies include a very large reactivity bias for high-void BWR fuels,

relatively large group-wise reaction rate errors, large reactivity bias at moderate and high burnup points, sensitivity to the number of radial rings, cold-to-hot reactivity swings and no available ENDF/B-VII.1 library. The new MPACT 51-group libraries have been developed to resolve these issues.

This paper describes the detailed procedure used to generate the new v4.2m2 MPACT 51-group libraries with ENDF/B-VII.0 and VII.1 and provides various benchmark results that demonstrate improvements in the new libraries compared with the v4.1m3 MPACT 47-group library with ENDF/B-VII.0.

### II. LIBRARY GENERATION

#### 1. MPACT Library Generation

The MPACT multigroup (MG) library generation procedure includes eight steps. (a) The AMPX MG library is generated by using temperature-dependent pointwise (PW) weighting functions, which are obtained from the CENTRM [3] PW slowing-down transport calculations. Resonance data are generated by narrow resonance (NR) approximation. (b) Intermediate resonance (IR) parameters are generated, and resonance data are updated with new data, which are obtained by the CENTRM homogeneous slowing-down calculations using LAMBDA and IRFFACTOR-hom [3], as shown in Figure 1. (c) Resonance data are updated with new data calculated by the CENTRM heterogeneous slowing-down calculations for important resonance nuclides by using IRFFACTOR-het [3]. (d) Subgroup data are generated for the selected nuclides by using SUBGR [3]. (e) Epithermal upscattering resonance and subgroup data are generated for  $^{238}\text{U}$  by using the continuous energy SCALE Monte Carlo code CE-KENO [3], the embedded self-shielding method [5] and SUBGR.

This manuscript has been authored by UT-Battelle, LLC, under Contract No. DE-AC0500OR22725 with the U.S. Department of Energy. The United States Government retains and the publisher, by accepting the article for publication, acknowledges that the United States Government retains a non-exclusive, paid-up, irrevocable, world-wide license to publish or reproduce the published form of this manuscript, or allow others to do so, for the United States Government purposes. The Department of Energy will provide public access to these results of federally sponsored research in accordance with the DOE Public Access Plan (<http://energy.gov/downloads/doe-public-access-plan>).

(f) Transport correction factors are generated for  $^1\text{H}$  by performing a fixed-source transport calculation. (g) MG background cross sections are obtained for most nuclides and to collect transient data. (h) The final step is to generate the final MPACT MG library with the data prepared at steps (a) through (g) by using DECLIB.

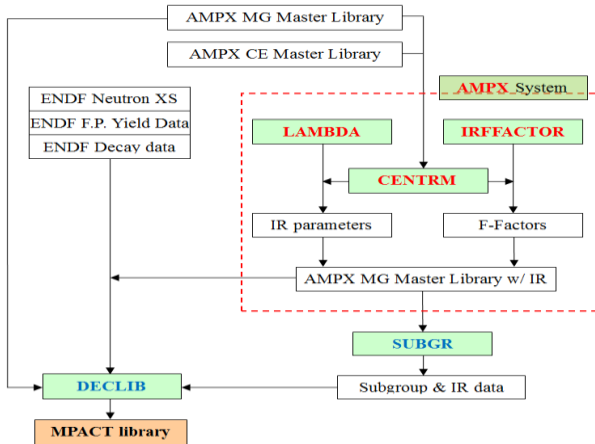


Fig. 1. Flow chart to generate resonance data

The MPACT 51-group libraries differ from the MPACT 47-group libraries following the following ways:

- New weighting PW function to improve cold-to-hot reactivity swing,
- New 51-group structure based on the SCALE 6.2 252-group structure,
- Transport correction factors obtained by using SCALE-XSDRN  $S_N$  calculations,
- No sensitivity on the number of radial rings,
- Superhomogenization (SPH) factor applications to important  $^{238}\text{U}$  resonances,
- Improvement in burnup calculations, and
- Generated for both ENDF/B-VII.0 and VII.1 libraries.

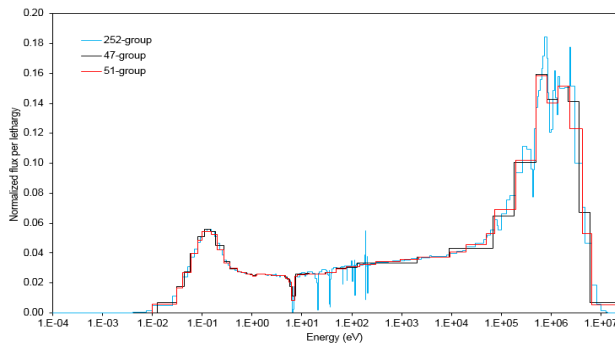


Fig. 2. Comparison of energy group structures

## 2. New 51-Group Structure

The MPACT 47-group structure was from the HELIOS-1.9 [6] 47-group structure, which includes very

wide energy groups in the range of 100 eV to 100 keV, which results in significant reaction rate differences for high-void BWR cases. The new 51-group structure was developed by adding 4 more groups to the 47-group structure and by adjusting group boundaries to be consistent with the 252-group structure. Figure 2 provides a comparison of 47-, 51- and 252-group structures.

## 3. SPH Factor Generation

Figure 3 describes a procedure to obtain the SPH factor for  $^{238}\text{U}$  to conserve reaction rates between the CE-KENO reference solutions and the MPACT results for which the CE-KENO models include the same variation cases as the heterogeneous IRFFACTOR cases. The SPH factors can be selectively applied to the specified energy groups indicating significant reaction rate differences. Figure 4 compares reaction rate differences for  $^{238}\text{U}$  with and without SPH factors. The differences are obtained from a comparison between the MPACT and CE-KENO reaction rates. The result indicates significant improvements in the largest resonance and high-energy resonances.

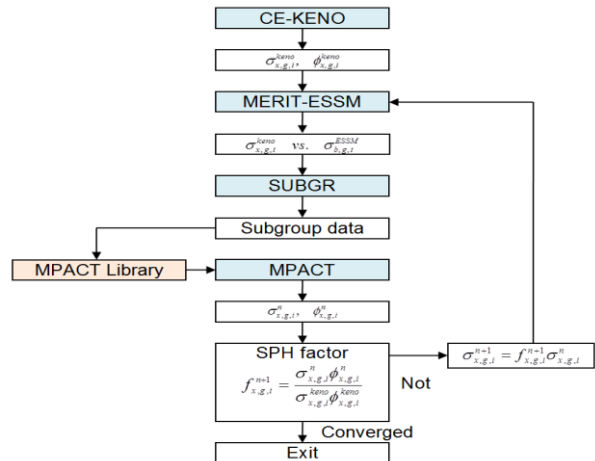


Fig. 3. Procedure to generate the SPH factors

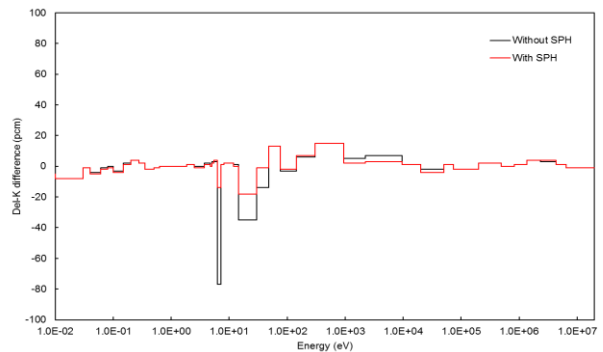


Fig. 4.  $^{238}\text{U}$  group-wise absorption reaction rate differences with and without SPH factors

#### 4. Transport Correction Factors

Transport correction factors for  $^1\text{H}$  based on the Neutron Leakage Conservation (NLC) method [7] have been generated by using 1-D Method of Characteristics (MOC) program. A new procedure, HTransportXS, which is based on SCALE-XSDRN with discrete ordinate ( $S_N$ ) diamond differencing (DD), has been developed. When  $S_N$  DD is used, HTransportXS can obtain the converged solution with fewer spatial meshes than MOC. Table 1 provides the converged options of the number of spatial meshes, quadrature order, and scattering order for 1-D MOC and DD.

Table 1. Optimized modeling options

Case	Width (cm)	# of meshes	Quadrature order	Scattering order
MOC1D	100.0	20000	$S_{16}$	$\geq P_3$
HTransportXS	100.0	500	$S_{64}$	$P_5$

In Figure 5, the comparison of transport correction factors between MOC and DD indicates some differences at epithermal energy groups. Benchmark calculations have been performed for the CASL VERA progression problems 1, 2, and 5 [8]. The eigenvalue differences ( $\Delta k$ ) are less than 2 pcm and 12 pcm for single-pin and assembly problems, respectively, and the pin power differences for assemblies are less than 0.08%. Table 2 provides a comparison of the multiplication factors and pin power distributions for problems 1, 2, and 5, which include pin, assembly, and 2-D PWR whole core problems with and without control rod insertions. The  $\Delta k$  differences are less than 2.6 pcm, and the maximum pin power differences are less than 0.08%. The  $^1\text{H}$  transport correction factors could be obtained by very simple  $S_N$  DD differencing.

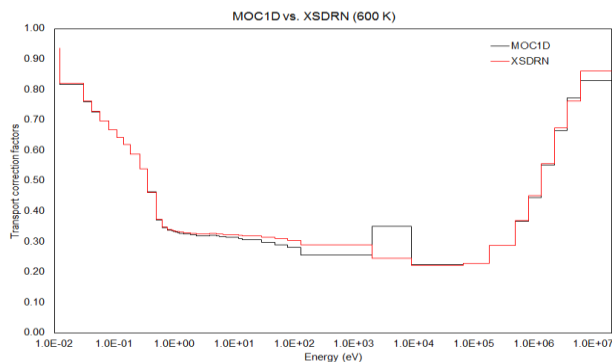


Fig. 5. Comparison of transport correction factors

#### 5. Sensitivity on the Number of Radial Rings

The MPACT 47-group library shows a sensitivity to the number of radial rings; a nonphysical amount of reactivity differences is introduced at around 250 pcm between 1 and 10 radial rings, as shown in Figure 6. This issue resulted from the four-group subgroup levels to be used in obtaining

background cross sections for seven-group subgroup calculations. As shown in Figure 6, the four-group subgroup levels are newly optimized to have significantly reduced sensitivity in the MPACT 51-group libraries.

Table 2. Results of the sensitivity calculation

Problems		$\Delta k$ (pcm)	Pin power diff. (%)	
			Max.	RMS
Pin	1A	1.4	-	-
	1B	1.5	-	-
	1C	1.6	-	-
	1D	1.7	-	-
	1E	0.5	-	-
Assembly	2A	1.1	0.008	0.004
	2B	1.0	0.007	0.004
	2C	1.0	0.008	0.004
	2D	1.1	0.008	0.004
	2E	-0.2	0.005	0.003
	2F	-1.0	0.010	0.002
	2G <sup>a</sup>	-4.8	0.016	0.007
	2H <sup>b</sup>	-11.8	0.035	0.014
	2I	1.1	0.007	0.004
	2J	-0.9	0.006	0.002
	2K	-0.8	0.010	0.002
	2L	0.6	0.011	0.004
	2M	0.4	0.010	0.004
	2N	-0.7	0.007	0.003
2O	-0.9	0.008	0.004	
2P	-1.9	0.009	0.005	
2Q	0.1	0.008	0.004	
2D core	5A	-1.7	0.077	0.032
	5B	-2.3	0.082	0.040
	5C	-2.6	0.079	0.038

<sup>a</sup>AgInCd control rod

<sup>b</sup>B<sub>4</sub>C control rod

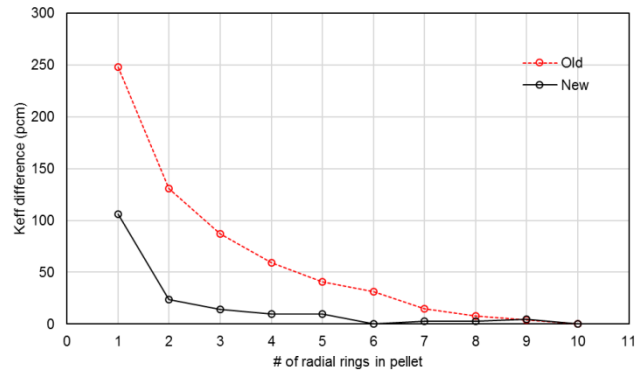


Fig. 6. Sensitivity of the number of radial rings in pellet

### III. CALCULATION AND RESULTS

#### 1. VERA Progression Benchmark Problems

Table 3 provides VERA progression benchmark problems [8], including single pins and assemblies; assembly layouts are shown in Figure 7.

Tables 4 and 5 summarize benchmark results for the VERA progression problems calculated by using the ENDF/B-VII.1 MPACT 51-group library with and without considering  $^{238}\text{U}$  epithermal upscattering, respectively. Maximum  $k_{\text{eff}}$  differences are shown in AIC control rod insertion cases.

Table 3. VERA progression benchmark problems

Case	Description	$^{235}\text{U}$	Mod/Fuel	$\text{g}/\text{cm}^3$
1A	pin	3.1	565/565	0.743
1B	pin	3.1	600/600	0.661
1C	pin	3.1	600/900	0.661
1D	pin	3.1	600/1200	0.661
1E	pin + IFBA	3.1	600/600	0.743
2A	FA, no BP	3.1	565/565	0.743
2B	FA, no BP	3.1	600/600	0.661
2C	FA, no BP	3.1	600/900	0.661
2D	FA, no BP	3.1	600/1200	0.661
2E	FA + 12 Pyrex	3.1	600/600	0.743
2F	FA + 24 Pyrex	3.1	600/600	0.743
2G	FA + 24 AIC CR	3.1	600/600	0.743
2H	FA + 24 B4C CR	3.1	600/600	0.743
2I	FA + Instrument Thimble	3.1	600/600	0.743
2J	FA + Instrument Thimble + 24 Pyrex	3.1	600/600	0.743
2K	FA + Zoned enrichment + 24 Pyrex	3.1/3.6	600/600	0.743
2L	FA + 80 IFBA	3.1	600/600	0.743
2M	FA + 128 IFBA	3.1	600/600	0.743
2N	FA + 104 IFBA + 20 WABA	3.1	600/600	0.743
2O	FA + 12 Gadolinia	1.8/3.1	600/600	0.743
2P	FA + 24 Gadolinia	1.8/3.1	600/600	0.743

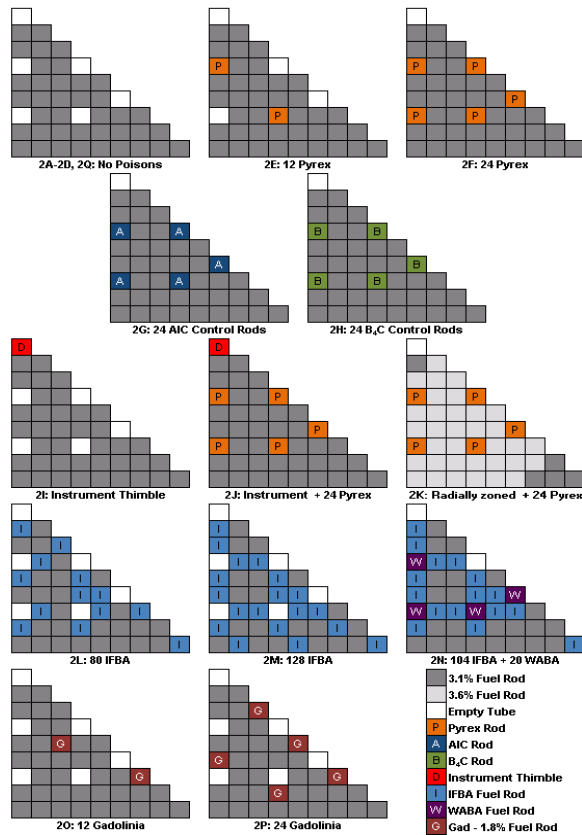


Fig. 7. Problem 2 lattice layouts

Table 4. Benchmark results (ENDF/B-VII.1 MPACT 51-g library, no  $^{238}\text{U}$  epithermal upscattering)

Case	CE-KENO		MPACT P2			
	$k_{\text{eff}}$	S.D.	$k_{\text{eff}}$	$\Delta k$ pcm	Pin power %	
					S.D.	Max.
1A	1.18698	0.00011	1.18751	-53		
1B	1.18209	0.00009	1.18258	-49		
1C	1.17152	0.00008	1.17156	-4		
1D	1.16246	0.00009	1.16225	21		
1E	0.77158	0.00010	0.77311	-153		
2A	1.18191	0.00008	1.18256	-65	0.12	0.24
2B	1.18307	0.00009	1.18343	-37	0.12	-0.27
2C	1.17358	0.00010	1.17336	22	0.11	0.28
2D	1.16531	0.00010	1.16484	47	0.12	0.39
2E	1.06933	0.00009	1.06992	-59	0.13	-0.37
2F	0.97598	0.00009	0.97635	-38	0.15	0.40
2G	0.84799	0.00008	0.84990	-192	0.26	0.61
2H	0.78810	0.00012	0.78882	-72	0.22	-0.61
2I	1.17969	0.00008	1.18029	-60	0.13	0.31
2J	0.97503	0.00010	0.97560	-57	0.17	-0.39
2K	1.01961	0.00010	1.02062	-101	0.14	0.36
2L	1.01856	0.00010	1.01905	-49	0.12	0.33
2M	0.93861	0.00009	0.93910	-50	0.15	-0.32
2N	0.86962	0.00008	0.86974	-12	0.20	0.59
2O	1.04726	0.00010	1.04676	50	0.15	-0.37
2P	0.92668	0.00010	0.92558	110	0.16	-0.40

Table 5. Benchmark results (ENDF/B-VII.1 MPACT 51-g library,  $^{238}\text{U}$  epithermal upscattering)

Case	CE-KENO		MPACT P2			
	$k_{\text{eff}}$	S.D.	$k_{\text{eff}}$	$\Delta k$ pcm	Pin power %	
					S.D.	Max.
1A	1.18603	0.00010	1.18602	1		
1B	1.18094	0.00009	1.18094	0		
1C	1.16946	0.00009	1.16900	46		
1D	1.15925	0.00009	1.15857	68		
1E	0.77099	0.00010	0.77220	-121		
2A	1.18099	0.00009	1.18122	-23	0.10	-0.28
2B	1.18225	0.00009	1.18194	31	0.11	-0.23
2C	1.17169	0.00008	1.17105	64	0.12	-0.27
2D	1.16252	0.00009	1.16152	100	0.10	0.31
2E	1.06840	0.00008	1.06866	-26	0.12	-0.26
2F	0.97501	0.00010	0.97518	-17	0.17	-0.38
2G	0.84716	0.00009	0.84892	-176	0.25	0.51
2H	0.78768	0.00010	0.78793	-24	0.22	0.55
2I	1.17858	0.00008	1.17891	-33	0.11	0.25
2J	0.97424	0.00009	0.97443	-19	0.13	-0.29
2K	1.01901	0.00010	1.01941	-40	0.17	0.33
2L	1.01774	0.00009	1.01788	-15	0.14	0.34
2M	0.93803	0.00011	0.93804	-1	0.11	-0.23
2N	0.86882	0.00009	0.86875	8	0.17	0.42
2O	1.04643	0.00010	1.04555	88	0.13	-0.30
2P	0.92611	0.00010	0.92452	159	0.17	-0.44

There is a bias of about 50 pcm in  $k_{eff}$  differences between the results with and without considering  $^{238}\text{U}$  epithermal upscattering. The bias can be from approximation of the Bondarenko iteration to consider resonance interference and truncation error in generating data for the resonance table and subgroups by using heterogeneous models. The maximum standard deviations of the pin power differences are 0.26% and 0.25%, and the maximum pin power differences are 0.61% and 0.55% for both options.

Table 6 provides comparisons of the ENDF/B-VII.1 results with the ENDF/B-VII.0 results obtained by performing the CE-KENO and MPACT calculations. ENDF/B-VII.0 and VII.1 introduce differences of less than 50 pcm except for a 2P assembly case bearing 24 gadolinia rods. The average CE-KENO results with ENDF/B-VII.0 overestimate  $k_{eff}$  by about 20 pcm; the average MPACT results show about 16 pcm overestimation in  $k_{eff}$ .

Table 6.  $k_{eff}$  difference between ENDF/B-VII.0 and VII.1

Case	CE-KENO			MPACT			a-b
	VII.0	VII.1	$\Delta k[a]$	VII.0	VII.1	$\Delta k[b]$	
1A	1.18704	1.18698	6	1.18754	1.18751	3	3
1B	1.18215	1.18209	6	1.18264	1.18258	6	1
1C	1.17172	1.17152	20	1.17217	1.17156	62	-41
1D	1.16260	1.16246	14	1.16256	1.16225	31	-17
1E	0.77169	0.77158	11	0.77294	0.77311	-17	28
2A	1.18218	1.18191	27	1.18265	1.18256	9	17
2B	1.18336	1.18307	29	1.18356	1.18343	12	17
2C	1.17375	1.17358	17	1.17401	1.17336	65	-48
2D	1.16559	1.16531	28	1.16522	1.16484	37	-9
2E	1.06963	1.06933	30	1.07000	1.06992	8	22
2F	0.97602	0.97598	4	0.97637	0.97635	1	3
2G	0.84770	0.84799	-29	0.85051	0.84990	61	-90
2H	0.78822	0.78810	12	0.78870	0.78882	-11	23
2I	1.17992	1.17969	23	1.18045	1.18029	16	7
2J	0.97519	0.97503	17	0.97561	0.97560	1	16
2K	1.02006	1.01961	45	1.02063	1.02062	1	44
2L	1.01892	1.01856	35	1.01910	1.01905	4	31
2M	0.93880	0.93861	19	0.93909	0.93910	-1	20
2N	0.86962	0.86962	-1	0.86967	0.86974	-8	7
2O	1.04773	1.04726	47	1.04699	1.04676	23	24
2P	0.92741	0.92668	73	0.92585	0.92558	28	45

## 2. Various $^{235}\text{U}$ enrichments and Burnt Fuel Problems

Because the VERA progression problems do not include various  $^{235}\text{U}$  enrichment and burnup compositions, additional benchmark problems have been developed to determine the sensitivities of the libraries to  $^{235}\text{U}$  enrichment and burnup. The benchmark problems are based on the VERA progression problems 1B and 1C. Table 7 provides list of new extended VERA benchmark problems.

Benchmark calculations were performed by using the v4.2m5 ENDF/B-VII.1 MPACT 51-g library. Table 8 summarizes the benchmark results, which indicate no  $^{235}\text{U}$

enrichment bias and acceptable prediction for burnt fuels (less than 110 pcm for all cases).

In Table 9 multiplication factors are compared between ENDF/B-VII.0 and VII.1 by using CE-KENO and MPACT. The CE-KENO results with ENDF/B-VII.1 overestimates  $k_{eff}$  at high burnup points compared to ENDF/B-VII.0. The MPACT results show a consistent trend with the CE-KENO results. Improvements over the v4.1m3 MPACT 47-g library could be achieved for burnup cases by improving resonance data of Pu isotopes and by obtaining much more reasonable self-shielded cross sections for fission product isotopes and nonresonance energy groups by using reasonable background cross sections.

Table 7. Extended VERA benchmark problems

Case	Description	$^{235}\text{U}$ w/o	Burnup (MWD/kgU)
1B-21	PWR pin $^{235}\text{U}$ 2.1 w/o	2.1	0
1B-26	PWR pin $^{235}\text{U}$ 2.6 w/o	2.6	0
1B-31	PWR pin $^{235}\text{U}$ 3.1 w/o	3.1	0
1B-36	PWR pin $^{235}\text{U}$ 3.6 w/o	3.6	0
1B-41	PWR pin $^{235}\text{U}$ 4.1 w/o	4.1	0
1B-46	PWR pin $^{235}\text{U}$ 4.6 w/o	4.6	0
1C-00	PWR pin 3-ring, full isotopes	3.1	0
1C-10	PWR pin 3-ring, full isotopes	3.1	10
1C-20	PWR pin 3-ring, full isotopes	3.1	20
1C-40	PWR pin 3-ring, full isotopes	3.1	40
1C-60	PWR pin 3-ring, full isotopes	3.1	60

Table 8. Extended VERA benchmark results

Case	No Epithermal Upscatt		Epithermal Upscatt	
	KENO	P2, pcm	KENO	P2, pcm
1C-21	1.07008	-46	1.06908	7
1C-26	1.13506	-69	1.13402	-13
1C-31	1.18199	-59	1.18087	-7
1C-36	1.22098	-58	1.21992	4
1C-41	1.25239	-75	1.25153	9
1C-46	1.27881	-51	1.27764	4
1C-00-3a	1.24699	48	1.24496	111
1C-10-3a	1.08728	-86	1.08541	-65
1C-20-3a	1.00259	-45	1.00111	-6
1C-40-3a	0.88304	34	0.88157	47
1C-60-3a	0.80899	22	0.80736	2

Table 9.  $k_{eff}$  difference between ENDF/B-VII.0 and VII.1

Case	CE-KENO			MPACT			a-b
	VII.0	VII.1	$\Delta k[a]$	VII.0	VII.1	$\Delta k[b]$	
1C-00	1.24716	1.24699	17	1.24724	1.24651	73	-56
1C-10	1.08701	1.08728	-27	1.08851	1.08814	37	-64
1C-20	1.00195	1.00259	-64	1.00266	1.00304	-38	-26
1C-40	0.88108	0.88304	-196	0.88104	0.88270	-166	-30
1C-60	0.80657	0.80899	-242	0.80616	0.80877	-261	19



### 3. Depletion benchmark

Depletion benchmark calculations were performed by using the VERA benchmark problems 2C and 2O by changing moderator density to be 0.7 g/cm<sup>3</sup>. The specific power density was set to 40 w/g-U, and, to have fair comparison, identical recoverable energies per fission for fissionable nuclides were used in the codes. Three and five equi-volume depletion zones were introduced, and the nonequilibrium Xenon option was selected.

Since there is a burden on computing time when using a full burnup chain that includes 2200 isotopes, we developed a simplified burnup chain that includes 255 isotopes not to have least impact on multiplication factors. Sensitivity calculations were performed by using full and simplified burnup chains for various depletion problems that involve UO<sub>2</sub> and gadolinia pin and fuel assemblies with no burnable poison, PYREX burnable poison, and integral fuel burnable absorber (IFBA) burnable poison. Figure 8 provides differences of multiplication factors in pcm for the test cases. All the results with simplified burnup chains, except for the results for a gadolinia rod, are very consistent with those with full burnup chains (within 50 pcm at all burnup points). Even though the gadolinia rod is the most severe case and shows the largest difference, a fuel assembly with gadolinia rods shows good consistency.

Figures 9 and 10 show comparisons of multiplication factors as a function of burnup for fuel assemblies with UO<sub>2</sub> fuels and 12 gadolinia rods. The VERA-CS results with the v4.2m5 ENDF/B-VII.0 MPACT 51-g library are very consistent with the SERPENT [9] results (within 200 pcm at all burnup points).

A depletion  $k_{eff}$  comparison between ENDF/B-VII.0 and VII.1 is made for 1C in Figure 11. The  $k_{eff}$  differences in depletion between ENDF/B-VII.0 and VII.1 are very consistent with the results for the static burnt fuels shown in Table 8. The  $k_{eff}$  differences between 4.1m3 47-g and 4.2m5 51-g libraries, which range from 0 to 200 pcm, could be interpreted as improvements in the v4.2m5 MPACT 51-g libraries.

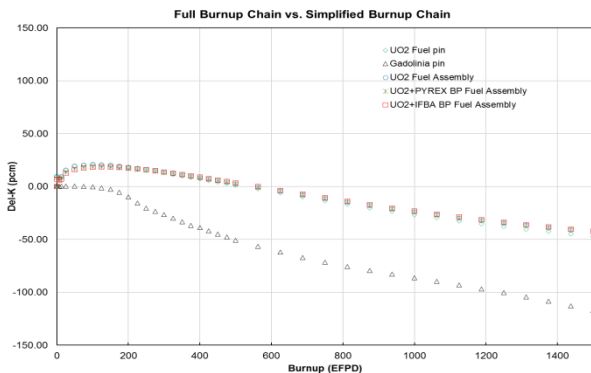


Fig. 8. Comparison of simplified burnup chain with full burnup chain

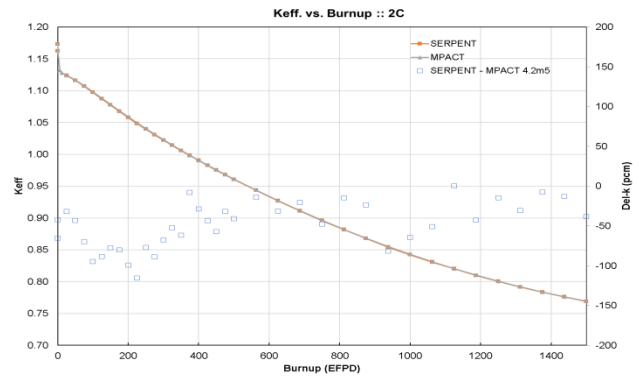


Fig. 9. Comparison of multiplication factors for case 2C

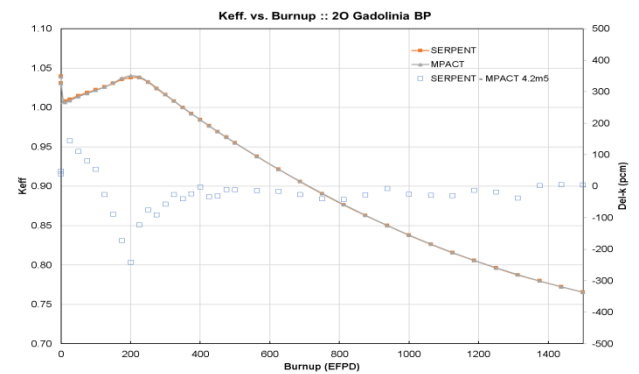


Fig. 10. Comparison of multiplication factors for case 2O

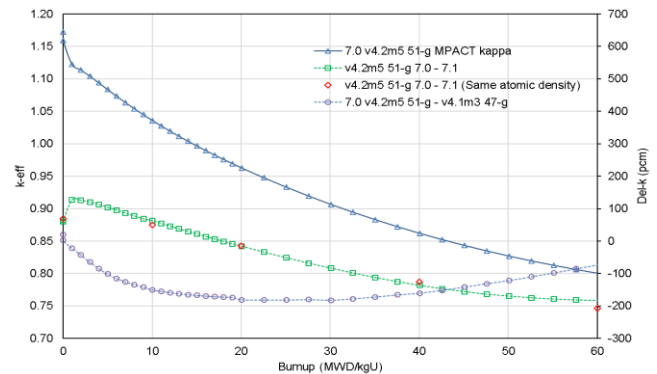


Fig. 11. Comparison of the multiplication factors

### IV. CONCLUSIONS

The v4.2m5 MPACT 51-group libraries with ENDF/B-VII.0 and VII.1 of which group structure is based on the SCALE 6.2 252-group structure have been successfully developed for the CASL MPACT neutronics simulator by using the AMPX/SCALE code packages. There are various improvements compared to the previous v4.1m3 MPACT 47-group library in many aspects, especially for burnup calculations, by optimizing self-shielded cross sections for

nonresonant nuclides and groupwise reaction rates by adopting SPH factors.

## **ACKNOWLEDGMENTS**

This research was supported by the Consortium for Advanced Simulation of Light Water Reactors ([www.casl.gov](http://www.casl.gov)), an Energy Innovation Hub (<http://www.energy.gov/hubs>) for Modeling and Simulation of Nuclear Reactors under US Department of Energy Contract No. DE-AC05-00OR22725.

## **REFERENCES**

1. MPACT: User's Manual Version 1.0.0, November 8, 2013.
2. "Consortium for Advanced Simulation of Light Water Reactors (CASL)." URL <http://www.casl.gov/> (2015).
3. "SCALE: A Modular Code System for Performing Standardized Computer Analyses for Licensing Evaluation," ORNL-TM/2005/39, Version 6.2, Oak Ridge National Laboratory, Oak Ridge, Tennessee (2016). (Available from Radiation Safety Information Computational Center at Oak Ridge National Laboratory as CCC-834.)
4. Kang Seog Kim, Mark L. Williams, Dorothea Wiarda, and Andrew T. Godfrey, "Development of a New 47-Group Library for the CASL Neutronics Simulators," M&C 2015, Nashville, TN, USA, April 19-23, 2015 (2015)
5. Mark L. Williams, Kang-Seog Kim, "The Embedded Self-Shielding Method," *PHYSOR 2012*, Knoxville, Tennessee, USA, April 15-20, 2012 (2012).
6. R. J. J. Stamm'ler et al., "The HELIOS Methods," Studsvik Scandpower (1998).
7. Bryan R. Herman, Benoit Forget, Kord Smith, "Improved Diffusion Coefficients Generated From Monte Carlo Codes," M&C 2013, Sun Valley, Idaho, May 5-9, 2013.
8. Andrew T. Godfrey, "VERA Core Physics Benchmark Progression Problem Specifications," CASL-U-2012-0131-004 rev.4, <http://www.casl.gov/publications.shtml> (2014).
9. J. LEPPANEN. "Serpent- a Continuous-energy Monte Carlo Reactor Physics Burnup Calculation Code", VTT Technical Research Centre of Finland (2012).